JACS
JOURNAL OF THE AMERICAN CHEMICAL SOCIETY
ARTICLE
pubs.acs.org/JACS

Mimicking the Silicon Surface: Reactivity of Silyl Radical Cations toward Nucleophiles

Bart Rijksen, Barend van Lagen, and Han Zuilhof*

Laboratory of Organic Chemistry, Wageningen University, Dreijenplein 8, 6703 HB Wageningen, The Netherlands

S *Supporting Information*

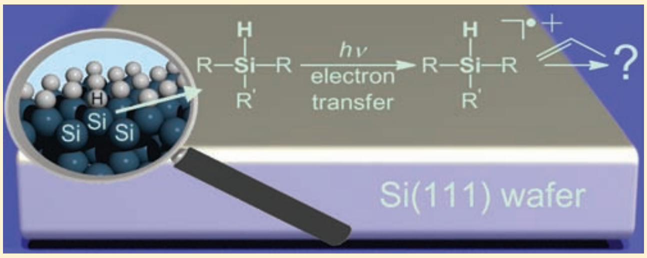

ABSTRACT: Radical cations of selected low molecular-weight silicon model compounds were obtained by photoinduced electron transfer. These radical cations react readily with a variety of nucleophiles, regularly used in monolayer fabrication onto hydrogen-terminated silicon. From time-resolved kinetics, it was concluded that the reactions proceed via a bimolecular nucleophilic attack to the radical cation. A secondary kinetic isotope effect indicated that the central Si—H bond is not cleaved in the rate-determining step. Apart from substitution products, also hydrosilylation products were identified in the product mixtures. Observation of the substitution products, combined with the kinetic data, point to an bimolecular reaction mechanism involving Si—Si bond cleavage. The products of this nucleophilic substitution can initiate radical chain reactions leading to hydrosilylation products, which can independently also be initiated by dissociation of the radical cations. Application of these data to the attachment of organic monolayers onto hydrogen-terminated Si surfaces via hydrosilylation leads to the conclusion that the delocalized Si radical cation (a surface-localized hole) can initiate the hydrosilylation chain reaction at the Si surface. Comparison to monolayer experiments shows that this reaction only plays a significant role in the initiation, and not in the propagation steps of Si—C bond making monolayer formation.

■ INTRODUCTION

Over the past two decades, extensive research has been performed on the formation of self-assembled organic monolayers on silicon and silicon-related surfaces. Typical examples are addition of alkenes and alkynes onto silicon[1−6] and germanium.[6,7] The passivation and functionalization of flat silicon surfaces has attracted a lot of attention because of their potential application in electronic devices.[2−4,6,8] In search of increasingly milder and faster attachment conditions, several fabrication methods were developed, making use of elevated temperatures,[9,10] UV irradiation,[11−14] hydrosilylation catalysts,[6,15,16] Grignard and alkyl lithium reagents,[17,18] electrochemistry,[19−21] and chemomechanical scribing.[22−25] These methods, however, still require a substantial input of energy to initiate monolayer formation, which can trigger side reactions. The search for lower energy input has led to the development of the mildest method yet for fabrication of high-quality monolayers, which can be performed at room temperature in the dark.[26] Recent studies showed that alkynes react faster than alkenes, and lead to higher packing densities.[27,28] Also the exclusion of oxygen during the fabrication process brings oxidation of the surface well below the detection limit of X-ray photoelectron spectrometry (XPS),[29] which opens the way for electronic devices.[30−35] However, the reaction times, in the range of hours, are too long for industrial application. To speed up monolayer formation, more detailed mechanistic knowledge is required.

For methods using UV irradiation ($\lambda < 350$ nm), it has been shown that a radical chain reaction is initiated by homolytic cleavage of Si—H bonds at the surface.[36] Recently, it was indicated that UV irradiation also causes photoemission of electrons from the Si surface into electron-acceptor levels in adjacent alkenes.[12] Mild attachment of 1-alkynes, however, takes place under conditions that will not allow regular crossing of high activation barriers, rendering direct cleavage of a Si—H bond unlikely. In earlier work from our lab, we proposed a mechanism[37] in which holes originating from excitons migrate to the surface forming delocalized radical cations. These radical cations are then attacked by nucleophiles. Upon alkylation, the resulting β-radical in the alkyl chain abstracts hydrogen atom from a neighboring Si—H site, leaving a radical at the silicon surface (Figure 1). A radical chain reaction similar to the mechanism described above is then initiated. This mechanism was further supported by island formation, observed with scanning tunneling microscopy (STM),[38−40] during monolayer fabrication. A dedicated mechanistic study of radical cation initiation via measurements and analysis of the kinetics has, however, not been undertaken yet.

The goal of the current work is to provide more detailed kinetic and product-based information regarding the reactivity of Si-based radical cations using small molecular models (Si_4, Si_7,

Received: December 2, 2010
Published: March 15, 2011

dx.doi.org/10.1021/ja110844e | *J. Am. Chem. Soc.* 2011, 133, 4998–5008

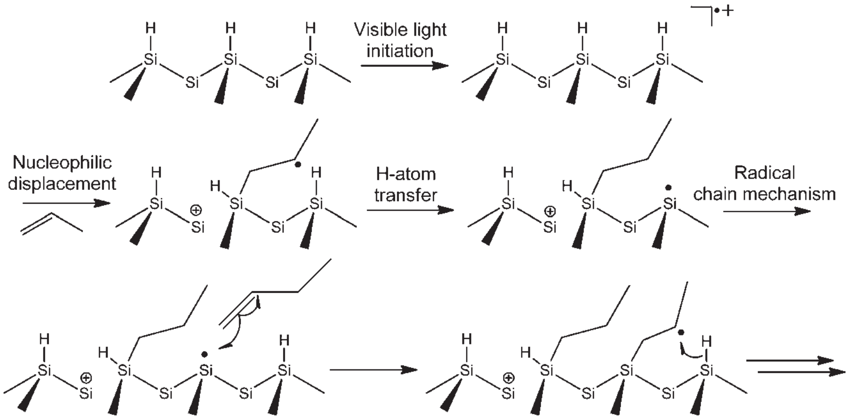

Figure 1. Monolayer formation onto H-terminated Si: radical cation-induced initiation,[37] followed by the radical chain mechanism.

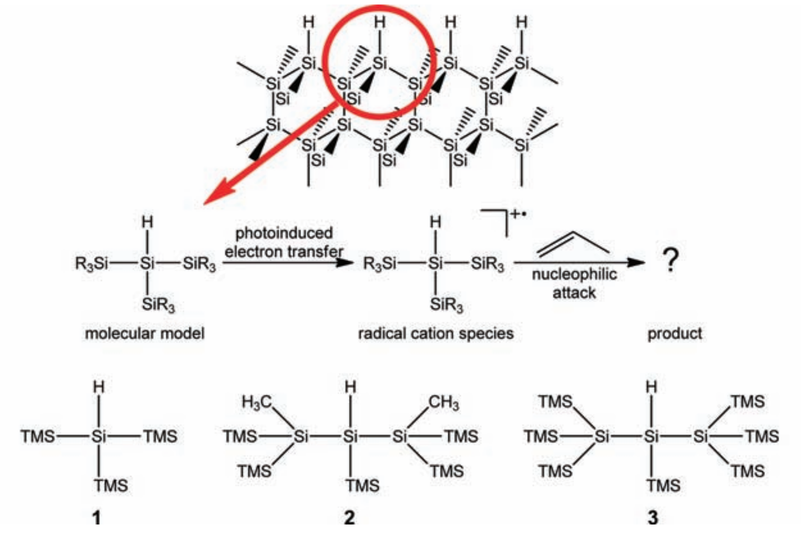

Figure 2. Representation of the selection of the models used in the current study (**1**−**3**) and the subsequent study of the silyl radical cations. Note: TMS = $Si(CH_3)_3$.

and Si_9 derivatives). Examples of radical cations of disilanes,[41,42] and cyclic and linear oligosilanes[43] are known in literature.[44] The models in this study, however, require a central Si−H site to mimic the top layer of the hydrogen-terminated silicon surface, and silicon atoms connected to this site to mimic the bulk (Figure 2, top). To our knowledge, radical cations of these branched silanes have not been studied before.

Tris(trimethylsilyl)silane (**1**), a Si_4 derivative, has proven its use in modeling surface reactions,[36,45,46] although the stability of the radical cation may be problematic due to its relatively small silicon backbone structure (branched Si_4; TMS = $Si(CH_3)_3$). Therefore, the model was extended by using a Si_3 structure with a central Si−H center, which was either appended with four or six TMS groups (compounds **2** and **3**, respectively; Figure 2, bottom), to combine a more extended delocalization with a tailor-made variation of the steric bulk around the Si−H site.

RESULTS AND DISCUSSION

1. Formation and Identification of Silyl Radical Cations.

Both **2** and **3** were synthesized according to modified literature procedures.[47] Silyl-potassium intermediates were prepared from tetrakis(trimethylsilyl)silane and methyl-tris(trimethylsilyl)-silane and potassium *tert*-butoxide.[48] Branched oligosilane structures were obtained by reaction of the resulting silyl-potassium building blocks with methyldichlorosilane. Efficient generation of the radical cations of **1**−**3** for time-resolved absorption measurements was achieved via photoinduced electron transfer using a positively charged sensitizer and toluene (1 M) as co-sensitizer: irradiation of *N*-methyl quinolinium (NMQ; 355 nm) in the presence of toluene yields the formation of toluene radical cation in high yields even in apolar solvents,[49] which can subsequently oxidize **1**−**3** to yield the silane radical cations $\mathbf{1}^{\bullet+}$, $\mathbf{2}^{\bullet+}$, and $\mathbf{3}^{\bullet+}$ (see Supporting Information for details). This method is highly superior over direct irradiation of the silanes, which yields significant amounts of photochemical side products, as below 300 nm photoionization competes with direct homolytic Si−H bond cleavage.

The oxidation potentials of **1**−**3** were obtained by cyclic voltammetry to ensure efficient electron transfer from the silanes to toluene$^{\bullet+}$ (E_{ox} (toluene) = 2.32 V vs Ag/AgCl).[50] From the results in Table 1, it becomes clear that all three compounds have a sufficiently lower oxidation potential than toluene (peak potentials E_p from 1.34 to 1.67 V vs Ag/AgCl). In more detail,

Table 1. Oxidation Potentials of Molecular Models 1, 2, and 3

	1	2	3
E_p[a]	1.67 ± 0.01	1.34 ± 0.01	1.42 ± 0.01
IP_{vert}[b]	190	172	173
$IP_{Koopmans}$[c]	154	143	146

[a] Peak potential in V vs Ag/AgCl (3 M KCl), 60 mv s^{-1}. [b] Vertical ionization potential (in kcal mol^{-1}; B3LYP/6-311++G(2d,2p)//B3LYP/6-311G(d,p) calculations); [c] Ionization potential according to Koopmans' theorem (in kcal mol^{-1}; B3LYP/6-311++G(2d,2p)//B3LYP/6-311G(d,p) calculations).

it shows that **1**, with the smallest silicon 'backbone', has the highest potential. Interestingly, **3** has a slightly higher oxidation potential than **2**, while having more silicon atoms. This may be explained by differences in the effective conjugation lengths, which is highly dependent on the conformation of the silicon backbone. Anticonformation of the silicon atoms contributes the most to conjugation, whereas small dihedral angles (syn to gauche) do not contribute significantly.[51] Because of steric hindrance of the bulky TMS groups, **3** cannot fully optimize the σ delocalization to the degree available for **2**. This steric effect is visible in the bond angle between the central Si and the two adjacent Si atoms. For **2** and **3**, this was calculated (B3LYP/6-311G(d,p)) to be 118° and 132° (experimental value: 128.3°),[47] respectively, that is, significantly larger than the 109° for unstrained sp^3 Si atoms. Calculated vertical ionization potentials (Table 1), obtained from the difference in absolute energies between the optimized neutral species and the corresponding radical cation in that geometry, confirm the significantly higher oxidation potential found for **1**. For **2** and **3**, the calculated potentials are close to each other, with the ordering in line with the experimental data. Finally, also the ordering of the ease of oxidation obtained using Koopmans' theorem[52] (Table 3, bottom row) correlates nicely with the oxidation potentials found.

The effect of the steric hindrance is also visible in Figure 3, which shows the relaxed geometries of the radical cations. In $\mathbf{1}^{\bullet+}$, two of the three Si−Si bonds are lengthened significantly more than the third bond (from 2.38 Å in the neutral precursor **1** to 2.50/2.50 and 2.40 Å, respectively). The charge is also predominantly present on the TMS moieties that are bound by a more lengthened Si−Si bond (from 0.027 in the precursor molecule **1** to 0.385 and 0.202 for the more and less lengthened Si−Si bonds, respectively). Also the angle ∠Si2−Si1−Si3 becomes smaller going from 113° to 99° as the radical cation is formed, while the other angles, ∠Si2−Si1−Si4 and ∠Si3−Si1−Si4, increase from 113° to 118°.

Also $\mathbf{2}^{\bullet+}$ (and $\mathbf{3}^{\bullet+}$) shows relaxation of the central angle ∠Si2−Si1−Si3, as it decreases from 118° (132°) to 107° (119°). Most charge is localized on the TMS groups that are part of the w-shaped silicon chain (e.g., Si5−Si2−Si1−Si3-Si7 in **2**). This is also shown by the Si−Si bond orders, which are about 0.77 in this chain and 0.89 for the remaining two Si−Si bonds. Also bond lengths are increased from 2.38 to 2.44 Å in this chain, whereas the other bonds are only marginally lengthened to 2.40 Å. The w-shape (dihedrals: 7−3−1−2, 143°; 3−1−2−5, 147°) is distinctive for the previously mentioned σ conjugation in silicon chains. Silicon atoms bound in this conformation can attribute to the conjugation and thus stabilize the molecule, while bonds that not significantly involved in the sigma conjugation are only slightly longer than in the neutral molecule (see Supporting Info for a more extensive discussion).

Time-resolved absorption measurements were performed in a laser transient absorption setup. To avoid interference of absorption of the NMQ radical, these experiments were performed in oxygen-saturated solutions of 1,2-dichloroethane (DCE) and hexafluoro-isopropanol (HFIP). Oxygen reacts rapidly with the NMQ radical (diffusion controlled) to photoinactive products. HFIP was reported to stabilize radical cations,[53] and silane radical cations specifically.[49] As shown in Figure 4 (left), toluene radical cation can be observed with absorption maxima at 425 and 825 nm. Upon addition of **3**, the absorption of toluene radical cation disappears, while a new transient appears at 690 nm. This indicates electron transfer between toluene radical cation and **3**. The transients resulting from **1**, **2**, and **3** (λ_{max} is 520, 670, and 690 nm, respectively) are depicted in Figure 4 (right). The stability of the transient in the presence of oxygen points toward a radical cationic transient, since organic radical cations typically react slowly with oxygen. To exclude the possibility of a radical mechanism, 1-bromohexane was added to the mixture, as bromoalkanes are known to react very fast with silicon-centered radicals.[7,54] This addition did not lead to any quenching and the lifetime of the transient remained the same, thus, excluding the involvement of a radical transient and supporting the assignment of the transients in Figure 4 (right) to $\mathbf{1}^{\bullet+}$, $\mathbf{2}^{\bullet+}$, and $\mathbf{3}^{\bullet+}$, respectively.

The radical cationic nature of these transients was further confirmed by investigating their ability to oxidize tris-*p*-tolylamine (TTA), a well-known electron donor with a low oxidation potential,[49] to yield the highly stable TTA radical cation (λ_{max} = 670 nm[55]). Directly after the laser pulse, electron transfer occurs primarily between sensitizer (7 mM) and the co-sensitizer toluene (1 M), because of their higher concentrations. Subsequently, toluene radical cation will quickly oxidize a silane, yielding a still relatively fast build-up of the silyl radical cation concentration and a simultaneous depletion of toluene radical cation. Under the conditions used, this process is finished after ca. 20 ns. Finally, after this process is nearly complete, TTA, which is present in a much lower concentration (1 μM), will transfer an electron to the silyl radical cations. As depicted in the left and right panels of Figure 5, a clear shift from 520 → 670 nm (from $\mathbf{1}^{\bullet+}$ to $TTA^{\bullet+}$) and 695 → 670 nm (from $\mathbf{3}^{\bullet+}$ to $TTA^{\bullet+}$), respectively, indicates electron transfer and TTA to $\mathbf{3}^{\bullet+}$. This confirms that the transients in Figure 4, right panel, can be attributed to the silyl radical cations.

2. Reactivity of Silyl Radical Cations. The lifetime of $\mathbf{1}^{\bullet+}$ was measured in an oxygen-saturated solution to minimize the interference of $NMQ^{\bullet}$, and was found to be 50 ± 5 ns. This proved to be too short to accurately determine the kinetics of reactions with nucleophiles using the current setup. Reproducibility of the lifetime measurements proved highly dependent on small amounts of water present. To prepare ultradry solutions, all samples were prepared under water-free conditions in a glovebox under argon atmosphere. The maxima of $\mathbf{2}^{\bullet+}$ and $\mathbf{3}^{\bullet+}$ did not overlap with the absorption of $NMQ^{\bullet}$, and the exclusion of oxygen did not affect the lifetimes. Under these conditions, the lifetimes for $\mathbf{2}^{\bullet+}$ and $\mathbf{3}^{\bullet+}$ were found to be 1250 ± 150 ns and 367 ± 17 ns, respectively. These lifetimes correlate with the ease of oxidation (Table 1) and the degree of delocalization that followed from the quantum chemical calculations: increased delocalization of the charge leads to decreased reactivity, that is, prolonged lifetime.

The rate of reaction of both transients was subsequently studied with a series of nucleophiles, which were selected based

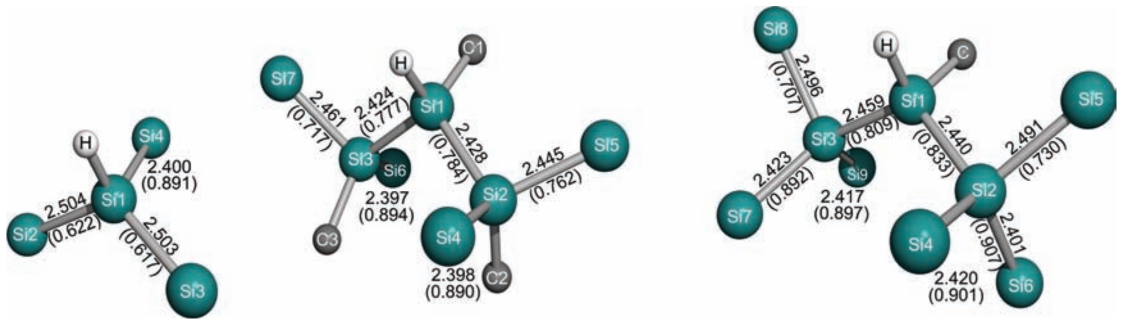

Figure 3. Silicon backbones and relevant carbon and hydrogen atoms of relaxed geometries of $1^{\bullet+}$, $2^{\bullet+}$, and $3^{\bullet+}$. Bond distances and Wiberg bond orders (between parentheses) are depicted near the corresponding bonds (B3LYP/6-311++G(2d,2p)//B3LYP/6-311G(d,p) calculations).

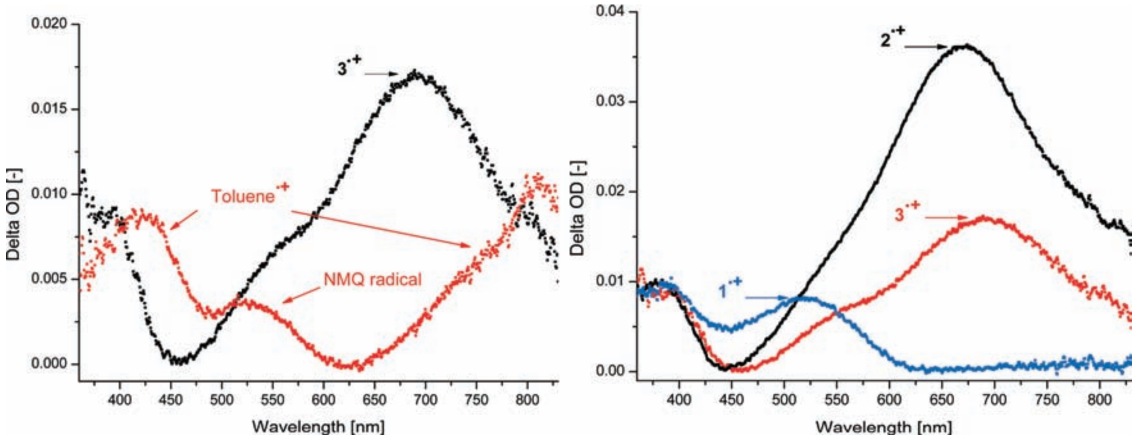

Figure 4. (left) UV−vis absorption spectra of the mixtures of NMQ (7 mM) and toluene (1.0 M) in 1,2-dichloroethane in presence (10 mM) and absence of **3** in the reaction mixture (50 ns after laser pulse at 355 nm). (right) UV−vis absorption spectra of $1^{\bullet+}$, $2^{\bullet+}$, and $3^{\bullet+}$ (50 ns after 355 nm laser pulse).

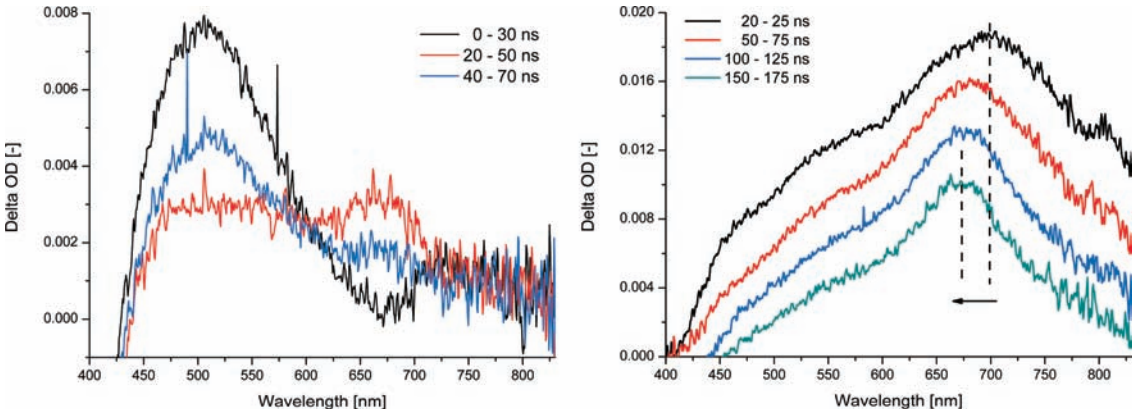

Figure 5. Absorption spectra of $1^{\bullet+}$ (left) and $3^{\bullet+}$ (right) in the presence of TTA recorded at increasing intervals after the laser pulse.

on their relevance for monolayer formation onto H-terminated silicon surfaces.[6] The decay of both transients was monoexponential (Figure 6, left), while the lifetimes of the radical cations became linearly shorter with increasing nucleophile concentration (Figure 6, right). This dependence on nucleophile concentration indicates a bimolecular reaction, since the silyl radical cation concentration is constant as this is only determined by the (near-constant) intensity of the laser pulse.

The reaction rate constants obtained from a Stern−Volmer type plot are pseudo-first-order constants (Table 2). From entries 1 and 2, it becomes clear that 1-alkynes react approximately a factor two faster with both silyl radical cations than 1-alkenes, which resembles the faster monolayer formation for 1-alkynes.[27−29] Entries 3−6 show that water, alcohols, acids and aldehydes, which are generally better nucleophiles than unsaturated carbons, react significantly faster with silyl radical

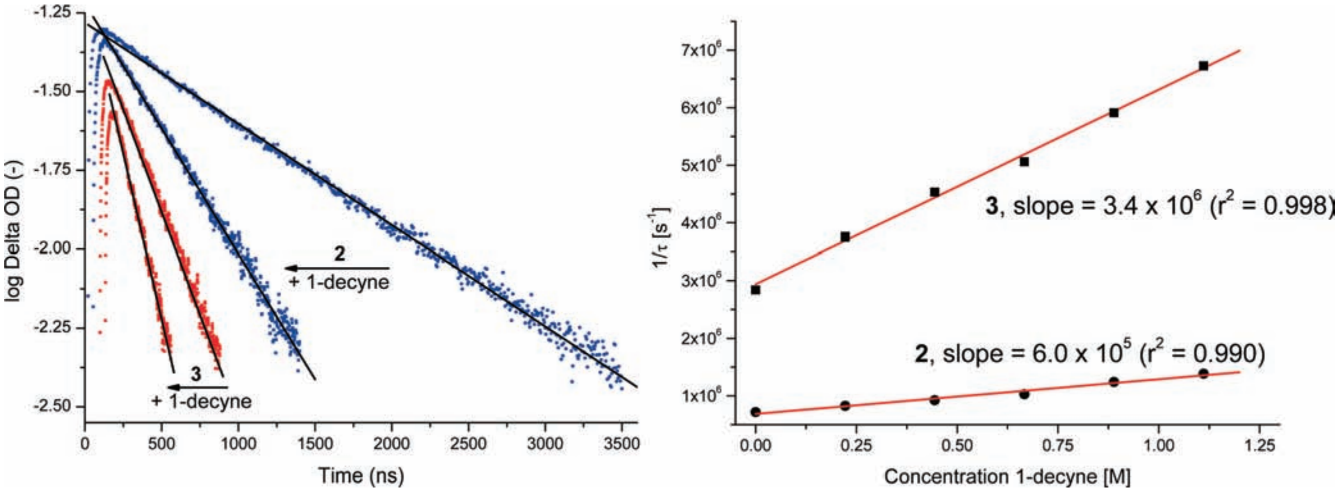

Figure 6. Decay of $2^{\bullet+}$ and $3^{\bullet+}$ in the absence or presence of 0.44 M 1-decyne (left) and; Stern−Volmer type plots obtained for $2^{\bullet+}$ and $3^{\bullet+}$ in the presence of 1-decyne (right).

Table 2. Pseudo-First-Order Rate Constants for the Reactions of $2^{\bullet+}$ and $3^{\bullet+}$ with Various Nucleophiles

entry	nucleophile	k_2[a]	k_3[a]
1	1-Decene	0.24 ± 0.02	1.7 ± 0.06
2	1-Decyne	0.61 ± 0.05	3.5 ± 0.2
3	H_2O	-	33 ± 0.2
4	1-Undecanol	9.7 ± 0.2	25 ± 0.4
5	1-Undecanal	22 ± 0.7	41 ± 2
6	1-Undecanoic acid	6.5 ± 0.04	22 ± 0.4
7	1-Decanethiol	-	>100[b]
8	1-Bromohexane	-	<0.1[c]
9	10-Undecenoic acid	-	25 ± 0.4
10	10-Undecynoic acid	-	21 ± 1
11	10-Undecenal	-	55 ± 1
12	10-Undecynal	-	45 ± 1

[a] Rates ± standard deviation (in 10^6 M^{-1} s^{-1}). [b] Rates too high to measure accurately with the setup used. [c] Rates too low to measure accurately with the setup used.

cations.[56,57] This increased reactivity of these nucleophiles is similar for $2^{\bullet+}$ and $3^{\bullet+}$, and nucleophilic attack onto the radical cation is further substantiated by the high reaction rate of 1-decanethiol with $3^{\bullet+}$. The significant difference in reactivity of $2^{\bullet+}$ and $3^{\bullet+}$ parallels the stability of the radical cations, and apparently outweighs the reduced steric hindrance around the Si−H site in $2^{\bullet+}$. As was discussed earlier, bromoalkanes (entry 8) show no significant reactivity toward the radical cations, excluding a radical reaction.

The high reactivity of alcohols, acids and aldehydes is, at first sight, not in line with monolayer-forming experiments, where these moieties are commonly used for further functionalization of the monolayers. Also the reactivity of water is striking, because it is commonly used to rinse hydrogen-terminated Si samples after etching steps. For a better comparison with these monolayer experiments, the reactivity of doubly functionalized alkenes and alkynes was tested, as can be seen in entries 9−12. From these results, it becomes clear that the reactivity of these doubly functionalized nucleophiles is similar to the reactivity of the monofunctionalized aldehydes and acids (Table 2, entries 5 and 6), and that the contribution of alkene and alkyne moieties is small. This implies that if the radical cation reaction would be the rate-limiting step in the attachment to the silicon surface, the monomers would attach via the aldehyde and acid functionalities rather than via the alkene or alkyne moieties. This is in contrast to what was found for example for aldehyde-functionalized monolayers prepared from ω-unsaturated-1-aldehydes.[58] These materials were reported to show 90% attachment via Si−C bonds, and only 10% attachment via Si−O−C bonds. Even more so, in the case of acid-functionalized monolayers, prepared from ω-unsaturated-1-acids, close to 100% attachment via Si−C bonds was reported.[59−62] According to these monolayer-forming experiments, at least the large majority of chains attaches via the alkene and alkyne moieties.

These data, thus, show that alkenes and alkynes do react rapidly with delocalized Si-centered radical cationic materials, which is consistent with efficient initiation of monolayer formation onto H-terminated Si via a Si-centered radical cation. In the case of Si surfaces, the absolute rates are, of course, expected to be significantly lower due the larger extent of delocalization, but the current experiments show that surface-localized radical cations on the H−Si surfaces can in principle initiate the reaction with 1-alkenes and 1-alkynes. The still much higher reaction rates of oxygen-centered nucleophiles with these Si-centered radical cations additionally show that, while initiation via this route may be feasible, the largest fraction of monolayer-forming molecules does not react via this mechanism, as this would yield extensive Si−O−C formation with ω-unsaturated-1-carboxylic acids and ω-unsaturated-1-aldehydes, which is not observed. The majority of Si−C bonds in a monolayer must therefore be formed via a different reaction.

To obtain more information about the exact reaction mechanism, kinetic isotope effects (KIEs) were studied. Therefore, the hydrogen at the central Si−H site of **3** was replaced by deuterium to give **3-D**. This did not cause noticeable changes in the absorption spectrum or in the lifetime of the radical cation in the absence of added nucleophiles. The results of the kinetics experiment of **3-D** with 1-decene and 1-decyne are depicted in Table 3. It becomes clear that the reactions of **3** are a factor 1.2 faster than reactions of **3-D**. This excludes Si−H bond cleavage

Table 3. Kinetic Isotope Effects for Reactions of $3^{\bullet+}$ with 1-Decene and 1-Decyne (in DCE/HFIP; 20 °C)

entry	nucleophile	k_{Si-H}[a]	k_{Si-D}[a]	KIE
1	1-Decene	1.72 ± 0.06	1.42 ± 0.17	1.21 ± 0.12
2	1-Decyne	3.53 ± 0.17	3.01 ± 0.28	1.17 ± 0.11

[a] Rates ± standard deviation (in 10^6 M^{-1} s^{-1}).

in the rate-determining step, as then typically a primary isotope effect with $k_H/k_D > 2$ would have been observed.[63] This thus also excludes a concerted mechanism with simultaneous Si—H bond cleavage and Si—C bond formation.[64] On the other hand, a KIE of 1.2 indicates a secondary kinetic isotope effect (SKIE), which places the hydrogen connected to the reaction center (α-position) or next to it (β-position). The SKIE can be caused by a change in hybridization, going from sp^3 to sp^2 in the transition state, or by hyperconjugation as deuterium is less able to stabilize the resulting cation. From these kinetic results, it is not possible to determine the exact reaction center, but Si—H bond cleavage in the TS of the substitution reaction is unlikely, which points to Si—Si cleavage as the bond-breaking process that accompanies Si—C bond formation.

3. Product Analysis. To substantiate this hypothesis, the reactivity of the radical cations of **1**—**3** was subsequently studied by their reaction with 1-decene and 1-decyne, and the reaction products were analyzed with GC—MS. Photochemical reactions ($\lambda_{exc} \geq 350$ nm) were performed in identical reaction mixtures (NMQ sensitized) as the transient absorption experiments. Product studies are typically performed with neutral sensitizers such as 9-cyanoanthracene and 9,10-diciyanoanthracene as they give less products of side reactions. However, it is well-documented that the nucleophilic reaction with the silyl radical cation competes with return electron transfer in the radical ion pair, resulting in the neutral sensitizer and silane.[65] In addition, it has been shown that disilanes are fragmented in a dissociative return electron transfer (DRET) process, resulting in the formation of radicals.[41] After confirming this for a 9-cyanoanthracene-sensitized test reaction (see below), we resorted to NMQ sensitization in these preparative reactions, specifically of **1**, as in the NMQ-sensitized reactions of **2** and **3** side reactions again precluded identification of reaction products resulting from nucleophilic attack. The reactions with **1** yielded reaction products in larger amounts, which could be analyzed and identified by GC—MS after independent synthesis of the most likely structures as reference compounds. Co-injection on the GC—MS and comparison of the mass spectra confirmed the identity of the products (Figure 7). The reaction of **1** with 1-decene resulted in a substitution of the silicon-bound hydrogen (**4a**) or a TMS group (**4b**) in a ratio of 2:1. The reaction of **1** with 1-decyne, yielded similar hydrosilylation (**5a**) and substitution products (**5b**) (Figure 7b). In addition, the ratio of cis/trans isomers was similar to the products of radical reactions performed with **1**.[45] This observation of **4a** and **5a** seems at variance with the findings of the kinetic study discussed earlier, as the secondary kinetic isotope effect indicates a bimolecular nucleophilic attack on the silicon backbone and rules out substitution of the Si—H in the reaction of the radical cations with nucleophiles. However, it is likely that **4a** and **5a** are the products of a hydrosilylation side reaction, which proceeds via a radical mechanism. In a 9-cyanoanthracene-sensitized test reaction with alkenes and alkynes, *only* hydrosilylation products **4a** and **5a** were found. This can be explained by DRET, which results in the efficient formation of silyl radicals that can subsequently react with unsaturated moieties. The absence of the substitution products in these product mixtures indicates that such substitution products are formed via a different route than a radical reaction, and the question arises whether the substitution products **4b** and **5b** are the result of a nucleophilic attack onto a radical cation.

To further distinguish between the radical and the radical cation reaction, the radical reaction was considered first. From the literature, it is known that silyl radicals react rapidly with alkenes[45] and even faster with bromine-containing compounds,[54] such as 1-bromohexane. To obtain a better insight, radical reactions of $\mathbf{1}^{\bullet}$ with 1-decene, 1-bromohexane and 1-undecanol were performed. A thermal radical initiator, 1,1′-azobiscyclohexanecarbonitrile, was used to generate $\mathbf{1}^{\bullet}$.[66] First, reaction with alkene did not result in any Si—Si cleavage (Figure 8a): only a hydrosilylation product was formed, which after co-injection proved to be identical to **4a**. In a second reaction, 1-bromohexane reacted very fast with $\mathbf{1}^{\bullet}$, resulting in exclusive formation of **6**. Again no products resulting from cleavage of the Si—Si bond were observed (Figure 8b). The third reaction of $\mathbf{1}^{\bullet}$ in the presence of 1-undecanol demonstrates that alcohols do not react with silyl radicals, since **8**, which was synthesized independently to function as reference compound, was completely absent from the reaction mixture (Figure 8c). The only product present in the mixture is the termination product (**7**) of two silyl radicals. To distinguish between radical and radical cation products, 1-undecanol was also reacted with $\mathbf{1}^{\bullet+}$, resulting in Si—Si cleavage products **9** and **10** (Figure 8d). These products can only be the result of a reaction with the silyl radical cation, as the previous reaction showed that 1-undecanol does not react with silyl radicals.

After identifying the trapping products of the silyl radical cation, it is possible to look more detailed at the substitution at the central Si atom. For alkenes and alkynes, it becomes clear that nucleophilic attack to the silyl radical cation results in dissociation and the formation of a TMS cation. The resulting β-carbon radical can subsequently initiate a radical chain reaction via abstraction of a hydrogen atom from a neighboring silane, yielding substitution products **4b** and **5b** and the silicon-centered radical $\mathbf{1}^{\bullet}$. In the case of 1-alkenes and 1-alkynes, the mechanism of this reaction is likely to be similar (Figure 9a,b). However, for alcohols, a different mechanism must be in effect since two substitution products (**9** and **10**) are observed. Nucleophilic attack on the central Si—H moiety in the radical cation leads loss of a TMS radical and formation of **9** (Figure 9c). However, attack on the TMS group will result in the formation of **10** and silyl radical **11** (Figure 9d). Routes 9c and 9d again show how a parallel radical chain reaction can be initiated. The observed 1:1 ratio of **9** and **10** suggests that both substitution pathways are in this case equally likely to occur.

These substitution reactions involving radical cations are much more facile than reactions that proceed via concerted Si—H bond cleavage and attachment of organic species onto the Si sites. For example, Chabal and co-workers studied the attachment of methanol onto H—Si(111) under prolonged heating at elevated temperature (65 °C, 12 h).[67] This reaction, which does not involve Si—Si bond cleavage, cannot take place under the currently studied reaction conditions given the calculated activation barrier of 33.7 kcal mol^{-1},[68] analogous to calculated barriers for the concerted attachment onto H—Si(111) of alkenes and alkynes (64.6 and 57.7 kcal mol^{-1}, respectively).[69] Estimates for

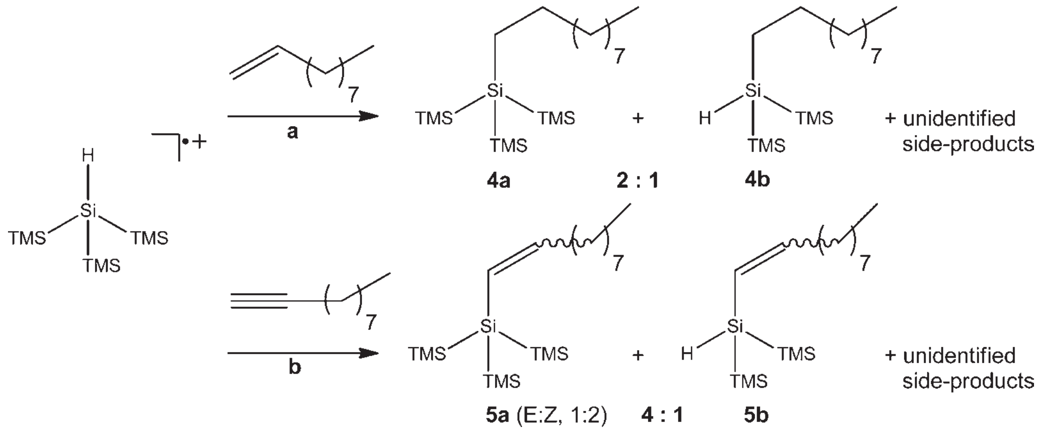

Figure 7. Products found in the reaction mixture for 1-decene (a) and 1-decyne (b).

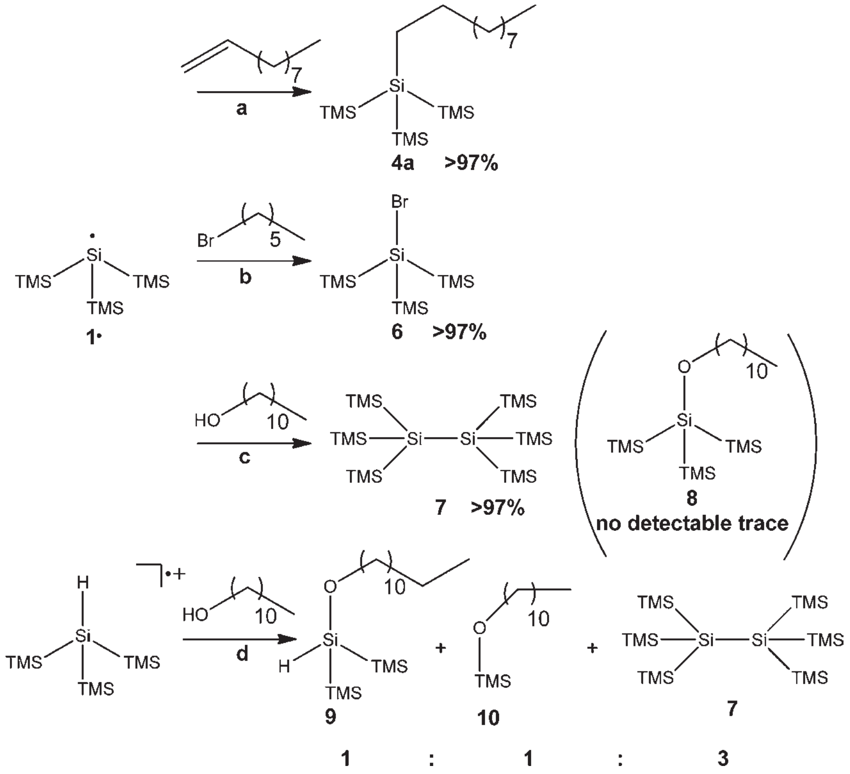

Figure 8. Products of reactions of $\mathbf{1}^{\bullet}$ (a−c) and of $\mathbf{1}^{\bullet+}$ with 1-undecanol (d).

the activation energies of reactions toward, for examle, silicon-based radical cation $\mathbf{3}^{\bullet+}$ range from 7 to 9 kcal/mol (see Supporting Information for more details), and thus indicate that the radical cation reactions proceed via a different, low activation-energy pathway.

Besides radical formation as a result of nucleophilic attack on the radical cation, also several other routes for initiation of the radical reaction could in principle be operative (see Figure 10). For instance, instability of $\mathbf{1}^{\bullet+}$ may result in spontaneous dissociation. Loss of H^+, resulting in the silicon-centered radical $\mathbf{1}^{\bullet}$ (Figure 10a), may be a viable option, although it can only occur as a side reaction, since otherwise products **9** and **10** would not predominantly form. A second option is the dissociation of a TMS^+ group, resulting in the silicon-centered radical $\mathbf{11}^{\bullet}$ (Figure 10b). The TMS^+ fragment would in turn react with 1-undecanol to form **10**, but the radical fragment cannot react with the alcohol to form **9**. Since both products **9** and **10** are present in equal amounts in the reaction mixture, also this pathway can only occur as a minor side reaction. The third possibility, a TMS radical splitting off, yielding the silicon-centered cation $\mathbf{11}^{+}$ is also unlikely (Figure 10c), as the resulting TMS radical would react rapidly with 1-decene, and the product of this reaction was not observed. Also this pathway would lead to unequal amounts of **9** and **10**, which is not the case, as described above. Finally, dissociation may also occur as a result of return electron transfer from the sensitizer to the silane (Figure 10d). As mentioned earlier, dissociative return electron transfer (DRET) is the major mechanism in the degradation of radical cations of

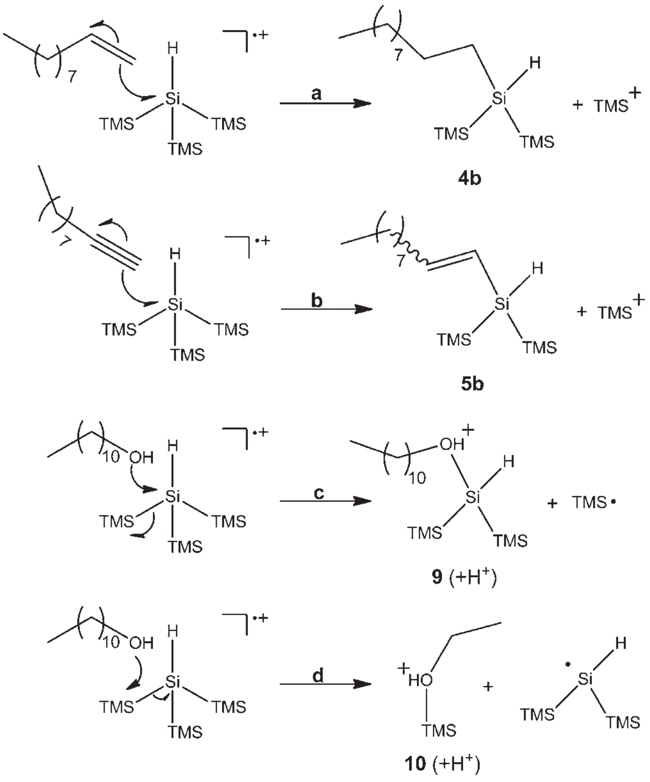

Figure 9. Reaction mechanisms of $\mathbf{1}^{\bullet+}$ with 1-decene (a), 1-decyne (b) and 1-undecanol (c and d).

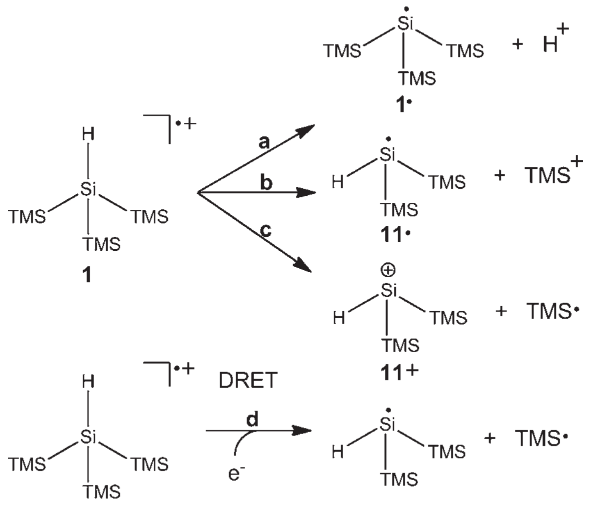

Figure 10. Dissociation pathways of $\mathbf{1}^{\bullet+}$ due to instability (a−c) or return electron transfer (d).

disilanes to monosilyl radicals.[41] Since this mechanism would also generate a TMS radical that should lead to products that were not observed, this mechanism is in our case unlikely as well. The above observations indicate that the Si radicals are predominantly formed by nucleophilic attack to the Si radical cation, rather than by spontaneous dissociation or DRET. This also demonstrates the feasibility of the formation of silicon-centered radicals at the silicon surface by nucleophilic attack to a delocalized radical cation. Such formation of radicals as a result of an initiating radical cation process has been hypothesized before,[37] and the data above provide further support for such a route. This more detailed mechanistic insight will be valuable to attempts to further improve monolayer formation onto hydrogen-terminated Si surfaces, both with respect to the rate of the reaction as well as in regard of the quality of the monolayer. Such studies are currently ongoing in our laboratories.

■ CONCLUSIONS

Small Si−H centered models (with 4, 7, and 9 Si atoms, respectively) were prepared and studied to gain insight in the mechanisms of formation of Si−C linked monolayers by 1-alkenes and 1-alkynes onto hydrogen-terminated silicon surfaces. Si-centered radical cations of these Si_4, Si_7, and Si_9 compounds react with high rates ($k_2 \sim 10^6\ M^{-1}\ s^{-1}$) in a bimolecular reaction with 1-alkynes and 1-alkenes, but do not react with 1-bromoalkanes. The reactivity with alkenes and alkynes is in line with initiation of Si−C linked monolayer formation by 1-alkenes and 1-alkynes onto H-terminated silicon surfaces via positively charged surfaces.[37] Such a bimolecular reaction is expected to yield a cation and a radical as products.

Better, oxygen-centered nucleophiles (aldehydes/carboxylic acids) react appreciably faster with the Si radical cations. These increasing reaction rates for stronger nucleophiles contrast with the small to insignificant reactivity of these moieties observed in the preparation of aldehyde-functionalized and acid-functionalized monolayers onto H-terminated Si. A radical cation mechanism does not account for the Si−C bond formation on H-terminated Si surfaces that is predominant also for ω-unsaturated 1-carboxylic acids and -1-aldehydes. This shows that the majority of monolayer-forming materials yields Si−C formation via another mechanism. The observation of hydrosilylation products for the model systems under current study indicates a radical side reaction. This radical formation proceeds predominantly via nucleophilic attack on the silyl radical cation, and only to a minor degree to spontaneous dissociation of the radical cations or dissociative return electron transfer. Radical cation-initiated attachment onto a H-terminated Si surface thus is the rate-limiting step in Si−C attached monolayer formation, but the majority of molecules is attached via a purely radical propagation reaction.

■ EXPERIMENTAL SECTION

Materials. Toluene and THF were distilled from CaH_2 and Na/benzophenone, respectively, before use. The nucleophiles that were commercially available were analyzed by GC−MS and did not need any further purification except for the aldehydes which were purified by column chromatography (Si-60, hexane/ethylacetate). 10-Undecynyl aldehyde was synthesized according to literature procedures.[70] Hexafluoro-iso-propanol (HFIP), 1,2-dichloroethane (DCE), and tris(trimethylsilyl)silane were used as obtained from Sigma-Aldrich. NMQ was synthesized according to a literature procedure,[49] and recrystallized before use. All solutions were stored over molecular sieves. All sample preparations were performed in a glovebox to ensure dry and oxygen-free conditions.

Equipment. Low-resolution mass spectra were obtained using an Agilent technologies 7890A GC, equipped with Alltech ATTM-5 ms column, in conjunction with a 5975C VL Mass Selective Detector. High-resolution mass spectra were obtained by direct probe measurements on a Fisons (VG) 7070. Nanosecond flash photolysis studies were carried out at 355 nm using the third harmonic of a Nd:YAG laser (Brilliant, Quantel, Inc.) Transient spectra were obtained with an LP920 spectrophotometer (Edinburgh Instruments Limited) fitted with a 450 W Xe arc lamp as probe-light source and a red-sensitive photomultiplier (R928, Hamamatsu) and ICCD camera (DH720, Andor technology) as detectors. All NMR spectra were recorded on a Bruker Avance III with an inverse broadband probe running at 400 MHz, with C_6D_6 as solvent.

Cyclic voltammograms were recorded on a μAutoLAB type III Potentiostat/Galvanostat (Eco Chemie BV). The working electrode consisted of an inlaid glassy carbon disk (2.0 mm diameter). A glassy carbon rod served as a counter electrode. To ensure nonaqueous conditions, a double junction Ag/AgCl electrode was used. The inner chamber was filled with a 3 M KCl solution and the outer chamber with 0.1 M tetrabutylammonium hexafluorophosphate in acetonitrile.

Transient Absorption Spectroscopy. For each data point, a 4 mL vial was filled with NMQ in DCE (0.8 mL 2.0 O.D. solution in DCE), silane (0.8 mL 40 mM in toluene), DCE (0.8 mL) and HFIP (1.6 mL) and the required amount of nucleophile (max. 100 μL). The sample was taken out of the glovebox immediately before starting the experiment. After loading the sample in a 5 mL syringe, it was connected to the flow cell in the laser setup. The cell was flushed with 1.5 mL of the sample and then the experiment was started. A typical data point was collected by averaging a series of six consecutive measurements which consisted of 12 scans and 12 background scans.

Calculations. All calculations were performed with the B3LYP functional,[71] using the Gaussian 09 suite of programs.[72] All geometries were optimized at the 6-311G(d,p) level and were shown to be global minima on the potential energy surface by frequency analysis. The energies were determined by single-point calculations at the 6-311++G(2d,2p) level and corrected with the zero-point energy determined from the 6-311G(d,p) geometry. The lowest-energy conformers for **2** and $\mathbf{2}^{\bullet+}$ were found by stepwise rotations of the TMS groups and preoptimizing at the B3LYP/3-21G level, before optimization of each rotamer at the B3LYP/6-311G(d,p) level of theory.

Cyclic Voltammetry. In a glovebox under argon atmosphere, a CV-cell was filled with a 5 mL solution of tetrabutylammonium hexafluorophosphate in acetonitrile (0.1 M). The counter and working electrode were placed and the cell was closed. After taking the cell from the box, it was immediately connected to a nitrogen line to keep the solution dry. The reference electrode, which was kept in dry acetonitrile stored over mol sieves, was placed in the CV cell under nitrogen flow. After recording the baseline, 40 μL of a silane solution in toluene (10 mM) was added with a syringe. Measurements were performed in single cycles.

Photochemistry Product Analysis. In a typical experiment for GC analysis, NMQ (0.5 mL 2.0 O.D. solution in DCE), *n*-decane (internal standard 5 μL), silane (0.5 mL of 40 mM in toluene) and nucleophile were mixed in a 4 mL vial with screwcap. The vial was then illuminated with a mercury lamp ($\lambda \approx 340$ nm) for the required time. Afterward, the mixture was analyzed by GC and GC−MS.

Radical Chemistry Product Analysis. In a typical experiment for GC analysis, 1̀,-azobiscyclohexanecarbonitrile (20 mg in 0.5 mL toluene), *n*-decane (internal standard 5 μL), silane (0.5 mL of 40 mM in toluene) and nucleophile were mixed in a 4 mL vial with screw cap. The vial was then placed in an oven at 100 °C for 1 h. Afterward, the mixture was analyzed by GC and GC−MS.

Syntheses. *Methyl-bis(methyl-bis[trimethylsilyl]silyl)silane* (**2**). This compound was synthesized following a modified literature procedure.[47] First, methyl-tris(trimethylsilyl)silane[73] and methyl-bis(trimethylsilyl)silyl-potassium[48] were prepared according to literature. The solvent was removed in vacuo and replaced by freshly distilled toluene. After cooling the mixture to −78 °C, a solution of dichloromethylsilane in toluene was added dropwise. The mixture was allowed to warm to room temperature and stirred for another 2 h. The product was purified by prep-HPLC (C18 reverse phase, methanol). ^{29}Si NMR (C_6D_6): −11.84 ($\underline{Si}(CH_3)_3 \sim 0.24$ (^{1}H)), −12.18 ($\underline{Si}(CH_3)_3 \sim 0.26$ (^{1}H)), −67.06 ($H\underline{Si}CH_3$), −83.16 ($\underline{Si}(TMS)_2CH_3$.

Methyl-bis(tris[trimethylsilyl]silyl)silane (**3**). This compound was synthesized following a modified literature procedure.[47] First, tetra(trimethylsilyl)silane[74] and tris(trimethylsilyl)silyl-potassium[48] were prepared according to literature. The solvent was removed in vacuo and replaced by freshly distilled toluene. After cooling the mixture to −78 °C, a solution of dichloromethylsilane in toluene was added dropwise. The mixture was allowed to warm to room temperature and stirred for another 2 h. The product was recrystallized from ethyl acetate/acetonitrile: ^{29}Si NMR (C_6D_6): −9.49 ($\underline{Si}(CH_3)_3$), −65.49 ($H\underline{Si}CH_3$), −124.61 ($\underline{Si}TMS_3$).

Deuterated Methyl-bis(tris[trimethylsilyl]silyl)silane (**3-D**). First, $[(Me_3Si)_3Si]_2SiHClMe$ was prepared from **3** according to a literature procedure.[75] In the subsequent step, this compound was reduced with an excess of $LiAlD_4$ in pentane until GC−MS showed complete conversion. The mixture was then filtrated over a silica plug and the solvent was evaporated, yielding pure **3-D**. ^{1}H NMR (400 MHz, C_6D_6): 0.35 (s, 54H), 0.59 (s, 3H); ^{13}C NMR (100 MHz, C_6D_6): −0.50 ($HSi\underline{C}H_3$), 3.48 ($Si(\underline{C}H_3)_3$); ^{29}Si NMR (C_6D_6): −9.35 ($\underline{Si}(CH_3)_3$), −24.73 ($\underline{Si}\text{-}(SiTMS_3)_3$), −65.89 ($D\underline{Si}CH_3$) . MS (EI) *m*/*z* (%): 524 (1) $[M^+ - CH_3]$, 464 (34) $[M^+ - HSi(CH_3)_3]$, 232 (56), 217(100), 73 (80) $[Si(CH_3)_3{}^+]$.

Decane-tris(trimethylsilyl)silane (**4a**), *Decane-bis(trimethylsilyl)silane* (**4b**). A solution of tris(trimethylsilyl)silane (0.5 g, 2.0 mmol) and potassium *tert*-butoxide (0.25 g, 2.2 mmol) in freshly distilled THF (5 mL) was stirred for 1 h at room temperature. A solution of 1-bromodecane (0.5 g, 2.3 mmol) in THF (5 mL) was added dropwise and the reaction was left to stir for another hour. After removal of the solvent, the solid residue was extracted with pentane, which after evaporation gave a colorless oil. The products were isolated with prep-HPLC (C-18 reverse phase, methanol). **4a:** Characteristics were similar to literature.[45] ^{29}Si NMR (C_6D_6): −13.22 ($\underline{Si}(CH_3)_3$), −82.11 ($\underline{Si}\text{-}TMS_3$). **4b:** ^{1}H NMR (400 MHz, C_6D_6): 3.90 (t, 1H), 1.51−1.58 (m, 2H), 1.29−1.40 (m, 14H), 0.86−0.93 (m, 5H), 0.23 (s, 18H); ^{13}C NMR (400 MHz, C_6D_6): 34.20, 32.69, 30.45, 30.43, 30.16, 30.12, 29.53, 23.46, 14.71, 7.87, 0.73. ^{29}Si NMR (C_6D_6): −15.87 ($\underline{Si}(CH_3)_3$), −66.66 ($\underline{Si}\text{-}TMS_2$). MS (EI) *m*/*z* (%): 316 (5) $[M^+]$, 301 (3) $[M^+ - CH_3]$, 242 (11) $[M^+ - HSi(CH_3)_3]$, 168 (31), 140 (36), 112 (33), 102 (74), 73 (100) $[Si(CH_3)_3{}^+]$. HR-MS (EI): 316.2442, calc. for $[M]^{+\bullet}$: 316.2438.

Decene-tris(trimethylsilyl)silane (**5a**). A solution of tris(trimethylsilyl)silane (1.0 g, 4.0 mmol), 1-decyne (2.5 mL, 14 mmol) and 1̀,-azobiscyclohexanecarbonitrile (0.25 g, 1.0 mmol) in heptane (20 mL) was refluxed for 2 h. Purification by flash column chromatography (C-18 reverse phase, methanol/MTBE) yielded a 1:1 mixture of cis/trans isomers. The isomers were isolated by prep-HPLC (C-18 reverse phase, methanol). HR-MS (EI): 386.2678, calc for $[M]^{+\bullet}$: 386.2677. (**E**): ^{1}H NMR (400 MHz, C_6D_6): δ 6.19 (m, 1H), 5.73 (d, 1H), 2.13 (q, 2H), 1.28−1.47 (m, 12H), 0.91 (t, 3H), 0.29 (s, 27H). ^{13}C NMR (400 MHz, C_6D_6): δ 150.46 (${=}\underline{C}H{-}CH_2$), 121.42 ($Si\text{-}\underline{C}H{=}$), 38.43, 32.62, 30.19, 30.13, 29.99, 29.77, 23.43,14.70 ($CH_2\text{-}\underline{C}H_3$), 1.42 ($Si(\underline{C}H_3)_3$). ^{29}Si NMR ($C_6D_6$): −13.24 ($\underline{Si}(CH_3)_3$), −86.18 ($\underline{Si}\text{-}TMS_3$). MS *m*/*z* (%): 386 (6) $[M^+]$, 371 (1) $[M^+ - CH_3]$, 313 (2) $[M^+ - Si(CH_3)_3]$, 297 (8), 174 (100) $[Si(Si(CH_3)_3)_2{}^+]$, 73 (63) $[Si(CH_3)_3{}^+]$. (**Z**): ^{1}H NMR (400 MHz, C_6D_6): δ 6.49 (q, 1H, *J* = 13 Hz), 5.67 (2t, 1H, *J* = 13 Hz), 2.19 (q, 2H), 1.28−1.45 (m, 12H), 0.91 (t, 3H), 0.29 (s, 27H). ^{13}C NMR (400 MHz, C_6D_6): δ 150.30 ($={}\underline{C}H{-}CH_2$), 120.32 ($Si\text{-}\underline{C}H{=}$), 36.56, 32.62, 30.64, 30.47, 30.44, 30.05, 23.43,14.70 ($CH_2\text{-}\underline{C}H_3$), 1.74 ($Si(\underline{C}H_3)_3$). ^{29}Si NMR ($C_6D_6$): −12.64 ($\underline{Si}(CH_3)_3$), −93.22 ($\underline{Si}\text{-}TMS_3$). MS (EI) *m*/*z* (%): 386 (7) $[M^+]$, 371 (1) $[M^+ - CH_3]$, 313 (2) $[M^+ - Si(CH_3)_3]$, 297 (9), 174 (100) $[Si(Si(CH_3)_3)_2{}^+]$, 73 (66) $[Si(CH_3)_3{}^+]$.

Decene-bis(trimethylsilyl)silane (**5b**, ***E/Z***). A mixture of decene-tris(trimethylsilyl)silane (0.6 mmol) and potassium *tert*-butoxide (0.6 mmol) in THF (0.5 mL) was stirred for 1 h at room temperature. Then, a cooled solution of 10% HCl in water (10 mL) was added and the mixture was stirred for another hour. The mixture was extracted with ether, and the combined organic fractions were dried over magnesium sulfate. Removal of the solvents gave a colorless oil which was purified by prep-HPLC (C-18 reverse phase, methanol). HR-MS (EI): 314.2277, calc for $[M]^{+\cdot}$: 314.2281. (**E**): ^{1}H NMR (400 MHz, C_6D_6): δ 6.28 (m, 1H, J = 18 Hz), 5.72 (m, 1H, J = 18 Hz), 3.81 (d, 1H, J = 5 Hz), 2.12 (q, 2H), 1.26−1.45 (m, 12H),0.91 (t, 3H), 0.25 (s, 18H). ^{13}C NMR (400 MHz, C_6D_6): 150.95, 119.99, 37.80, 32.28, 29.85, 29.75, 29.46, 29.38, 23.10, 14.35, 0.11. ^{29}Si NMR (C_6D_6): −15.71 ($\underline{Si}(CH_3)_3$), −70.20 ($\underline{Si}$-TMS_2). MS (EI) m/z (%): 314 (23) $[M^+]$, 299 (2) $[M^+ - CH_3]$, 255 (6) $[M^+ - HSi(CH_3)_3]$, 141 (43), 116 (69), 73 (100). (**Z**): ^{1}H NMR (400 MHz, C_6D_6): δ 6.52 (q, 1H, J = 13 Hz), 5.61 (m, 1H, J = 13 Hz), 3.90 (d, 1H, J = 8 Hz), 2.27 (q, 2H), 1.26−1.45 (m, 12H), 0.91 (t, 3H), 0.25 (s, 18H). ^{13}C NMR (400 MHz, C_6D_6): 150.28, 119.11, 34.19, 32.28, 30.08, 30.01, 29.80, 29.72, 23.10, 14.35, 0.11. ^{29}Si NMR (C_6D_6): −15.24 ($\underline{Si}(CH_3)_3$), −81.94 ($\underline{Si}$-TMS_2). MS (EI) m/z (%): 314 (24) $[M^+]$, 299 (2) $[M^+ - CH_3]$, 255 (7) $[M^+ - HSi(CH_3)_3]$, 141 (39), 116 (62), 73 (100).

*Undeca-oxy-tris(trimethylsilyl)silane (**8**).* In a 4 mL vial, chlorotris(trimethylsilyl)silane (0.25 g, 0.9 mmol) was dissolved in a mixture of pentane (1 mL) and triethylamine (2 mL). After addition of 1-undecanol (1 mL), the mixture was shaken and left at room temperature for 2 h. After removal of the solvents, the semisolid residue was extracted with pentane. Evaporation of the pentane yielded a colorless oil which was purified by flash-column chromatography (Si-60, hexane). ^{1}H NMR (400 MHz, C_6D_6): 3.58 (t, 2H), 1.56 (p, 2H), 1.28−1.41 (m, 16H) 0.92 (t, 3H), 0.30 (s, 27H). ^{13}C NMR (400 MHz, C_6D_6): 68.46, 33.59, 32.34, 30.14, 30.08 (2 C), 29.94, 29.81, 26.41, 23.12, 14.37, 0.58. ^{29}Si NMR (C_6D_6): 0.22 ($\underline{Si}$-TMS_3), −16.46 ($\underline{Si}(CH_3)_3$). MS (EI) m/z (%): 403 (8) $[M^+ - CH_3]$, 345 (8) $[M^+ - Si(CH_3)_3]$, 263 (100), 191 (48), 175 (39), 131 (24), 73 (69) $[Si(CH_3)_3{}^+]$. HR-MS (EI) $[M]^{+\cdot}$: 418.2941, calc for $[M]^{+\cdot}$: 418.2939.

*Undeca-oxy-tris(trimethylsilyl)silane (**9**).* MS (EI) m/z (%): 331 (2) $[M^+ - CH_3]$, 272 (2) $[M^+ - His(CH_3)_3]$, 159 (22), 117 (100), 73 (56).

■ ASSOCIATED CONTENT

S Supporting Information. Full citation of ref 72 (Gaussian 09), B3LYP/6-311G(d,p)-optimized geometries of silyl radical cations $\mathbf{1}^{\bullet+}$, $\mathbf{2}^{\bullet+}$, and $\mathbf{3}^{\bullet+}$, a more detailed discussion on the formation and characterization of $\mathbf{1}^{\bullet+}$, $\mathbf{2}^{\bullet+}$, and $\mathbf{3}^{\bullet+}$, and estimated activation barriers. This material is available free of charge via the Internet at http://pubs.acs.org.

■ AUTHOR INFORMATION

Corresponding Author

Han.Zuilhof@wur.nl

■ ACKNOWLEDGMENT

The authors thank Dr. Jacob Baggerman (Aquamarijn, BV) and Dr. Jos Paulusse (Wageningen University) for many fruitful discussions, Peter van Galen (Radboud University Nijmegen) for HR-MS measurements, and NanoNed, funded by the Dutch Ministry of Economic Affairs (Project WPC 7123), for financial support.

■ REFERENCES

(1) Ciampi, S.; Harper, J. B.; Gooding, J. J. *Chem. Soc. Rev.* **2010**, *39*, 2158.

(2) Boukherroub, R. *Curr. Opin. Solid State Mater. Sci.* **2005**, *9*, 66.

(3) Shirahata, N.; Hozumi, A.; Yonezawa, T. *Chem. Rec.* **2005**, *5*, 145.

(4) Wayner, D. D. M.; Wolkow, R. A. *J. Chem. Soc., Perkin Trans. 2* **2002**, 23.

(5) Sieval, A. B.; Linke, R.; Zuilhof, H.; Sudhölter, E. J. R. *Adv. Mater.* **2000**, *12*, 1457.

(6) Buriak, J. M. *Chem. Rev.* **2002**, *102*, 1271.

(7) Choi, K.; Buriak, J. M. *Langmuir* **2000**, *16*, 7737.

(8) Sieval, A. B.; Huisman, C. L.; Schoenecker, A.; Schuurmans, F. M.; Van der Heide, A. S. H.; Goossens, A.; Sinke, W. C.; Zuilhof, H.; Sudhölter, E. J. R. *J. Phys. Chem. B* **2003**, *107*, 6846.

(9) Linford, M. R.; Fenter, P.; Eisenberger, P. M.; Chidsey, C. E. D. *J. Am. Chem. Soc.* **1995**, *117*, 3145.

(10) Sieval, A. B.; Demirel, A. L.; Nissink, J. W. M.; Linford, M. R.; van der Maas, J. H.; de Jeu, W. H.; Zuilhof, H.; Sudhölter, E. J. R. *Langmuir* **1998**, *14*, 1759.

(11) Shestopalov, A. A.; Clark, R. L.; Toone, E. J. *Langmuir* **2010**, *26*, 1449.

(12) Wang, X. Y.; Ruther, R. E.; Streifer, J. A.; Hamers, R. J. *J. Am. Chem. Soc.* **2010**, *132*, 4048.

(13) Cicero, R. L.; Linford, M. R.; Chidsey, C. E. D. *Langmuir* **2000**, *16*, 5688.

(14) Terry, J.; Mo, R.; Wigren, C.; Cao, R. Y.; Mount, G.; Pianetta, P.; Linford, M. R.; Chidsey, C. E. D. *Nucl. Instrum. Methods Phys. Res., Sect B.* **1997**, *133*, 94.

(15) Buriak, J. M.; Stewart, M. P.; Geders, T.; Choi, H. C. *Abstr. Pap. Am. Chem. Soc.* **1999**, *218*, U457.

(16) Holland, J. M.; Stewart, M. P.; Allen, M. J.; Buriak, J. M. *J. Solid State Chem.* **1999**, *147*, 251.

(17) Hurley, P. T.; Nemanick, E. J.; Brunschwig, B. S.; Lewis, N. S. *J. Am. Chem. Soc.* **2006**, *128*, 9990.

(18) Juang, A.; Scherman, O. A.; Grubbs, R. H.; Lewis, N. S. *Langmuir* **2001**, *17*, 1321.

(19) Allongue, P.; de Villeneuve, C. H.; Pinson, J.; Ozanam, F.; Chazalviel, J. N.; Wallart, X. *Electrochim. Acta* **1998**, *43*, 2791.

(20) deVilleneuve, C. H.; Pinson, J.; Bernard, M. C.; Allongue, P. *J. Phys. Chem. B* **1997**, *101*, 2415.

(21) Robins, E. G.; Stewart, M. P.; Buriak, J. M. *Chem. Commun.* **1999**, 2479.

(22) Lee, M. V.; Guo, D. W.; Linford, M. R.; Zuilhof, H. *Langmuir* **2004**, *20*, 9108.

(23) Niederhauser, T. L.; Jiang, G. L.; Lua, Y. Y.; Dorff, M. J.; Woolley, A. T.; Asplund, M. C.; Berges, D. A.; Linford, M. R. *Langmuir* **2001**, *17*, 5889.

(24) Niederhauser, T. L.; Lua, Y. Y.; Jiang, G. L.; Davis, S. D.; Matheson, R.; Hess, D. A.; Mowat, I. A.; Linford, M. R. *Angew. Chem., Int. Ed.* **2002**, *41*, 2353.

(25) Yang, L.; Lua, Y. Y.; Lee, M. V.; Linford, M. R. *Acc. Chem. Res.* **2005**, *38*, 933.

(26) Scheres, L.; Arafat, A.; Zuilhof, H. *Langmuir* **2007**, *23*, 8343.

(27) Ng, A.; Ciampi, S.; James, M.; Harper, J. B.; Gooding, J. J. *Langmuir* **2009**, *25*, 13934.

(28) (a) Experimental: Scheres, L.; Giesbers, M.; Zuilhof, E. *Langmuir* **2010**, *26*, 10924. (b) Theoretical: Scheres, L.; Rijksen, B.; Giesbers, M.; Zuilhof, H. *Langmuir* **2011**, *27*, 972.

(29) Scheres, L.; Giesbers, M.; Zuilhof, H. *Langmuir* **2010**, *26*, 4790.

(30) Zigah, D.; Herrier, C.; Scheres, L.; Giesbers, M.; Fabre, B.; Hapiot, P.; Zuilhof, H. *Angew. Chem., Int. Ed.* **2010**, *49*, 3157.

(31) Popoff, R. T. W.; Asanuma, H.; Yu, H. Z. *J. Phys. Chem. C* **2010**, *114*, 10866.

(32) Campos, M. A. C.; Paulusse, J. M. J.; Zuilhof, H. *Chem. Commun.* **2010**, *46*, 5512.

(33) Yaffe, O.; Scheres, L.; Puniredd, S. R.; Stein, N.; Biller, A.; Lavan, R. H.; Shpaisman, H.; Zuilhof, H.; Haick, H.; Cahen, D.; Vilan, A. *Nano Lett.* **2009**, *9*, 2390.

(34) Seitz, O.; Vilan, A.; Cohen, H.; Hwang, J.; Haeming, M.; Schoell, A.; Umbach, E.; Kahn, A.; Cahen, D. *Adv. Funct. Mater.* **2008**, *18*, 2102.

(35) Seitz, O.; Bocking, T.; Salomon, A.; Gooding, J. J.; Cahen, D. *Langmuir* **2006**, *22*, 6915.

(36) Stewart, M. P.; Buriak, J. M. *J. Am. Chem. Soc.* **2001**, *123*, 7821.

(37) Sun, Q.-Y.; De Smet, L. C. P. M.; Van Lagen, B.; Giesbers, M.; Thuene, P. C.; Van Engelenburg, J.; De Wolf, F. A.; Zuilhof, H.; Sudhölter, E. J. R. *J. Am. Chem. Soc.* **2005**, *127*, 2514.

(38) Lopinski, G. P.; Wayner, D. D. M.; Wolkow, R. A. *Nature* **2000**, *406*, 48.

(39) Eves, B. J.; Sun, Q.-Y.; Lopinski, G. P.; Zuilhof, H. *J. Am. Chem. Soc.* **2004**, *126*, 14318.

(40) Cicero, R. L.; Chidsey, C. E. D.; Lopinski, G. P.; Wayner, D. D. M.; Wolkow, R. A. *Langmuir* **2002**, *18*, 305.

(41) Al-Kaysi, R. O.; Goodman, J. L. *J. Am. Chem. Soc.* **2005**, *127*, 1620.

(42) Guirado, G.; Haze, O.; Dinnocenzo, J. P. *J. Org. Chem.* **2010**, *75*, 3326.

(43) Karatsu, T.; Kanayama, K.; Takahashi, M.; Ishigohoka, N.; Fukui, K.; Kitamura, A. *Heteroat. Chem.* **2001**, *12*, 269.

(44) Karatsu, T. *J. Photochem. Photobiol., C* **2008**, *9*, 111.

(45) Kopping, B.; Chatgilialoglu, C.; Zehnder, M.; Giese, B. *J. Org. Chem.* **1992**, *57*, 3994.

(46) Sommer, L. H.; Pietrusza, E. W.; Whitmore, F. C. *J. Am. Chem. Soc.* **1947**, *69*, 188.

(47) Gross, T.; Reinke, H.; Oehme, H. *Can. J. Chem.* **2000**, *78*, 1399.

(48) Marschner, C. *Eur. J. Inorg. Chem.* **1998**, 221.

(49) Dockery, K. P.; Dinnocenzo, J. P.; Farid, S.; Goodman, J. L.; Gould, I. R.; Todd, W. P. *J. Am. Chem. Soc.* **1997**, *119*, 1876.

(50) Guirado, G.; Fleming, C. N.; Lingenfelter, T. G.; Williams, M. L.; Zuilhof, H.; Dinnocenzo, J. P. *J. Am. Chem. Soc.* **2004**, *126*, 14086.

(51) Krempner, C.; Reinke, H. *Organometallics* **2007**, *26*, 2053.

(52) Koopmans, T. *Physica* **1934**, *1*, 104.

(53) Eberson, L.; Hartshorn, M. P.; Persson, O. *J. Chem. Soc., Perkin Trans. 2* **1995**, 1735.

(54) Chatgilialoglu, C.; Griller, D.; Lesage, M. *J. Org. Chem.* **1989**, *54*, 2492.

(55) Shida, T. *Electronic Absorption Spectra of Radical Ions*; Elsevier: Amsterdam, The Netherlands, 1988.

(56) Todd, W. P.; Dinnocenzo, J. P.; Farid, S.; Goodman, J. L.; Gould, I. R. *J. Am. Chem. Soc.* **1991**, *113*, 3601.

(57) Dinnocenzo, J. P.; Simpson, T. R.; Zuilhof, H.; Todd, W. P.; Heinrich, T. *J. Am. Chem. Soc.* **1997**, *119*, 987.

(58) Hong, Q.; Rogero, C.; Lakey, J. H.; Connolly, B. A.; Houlton, A.; Horrocks, B. R. *Analyst* **2009**, *134*, 593.

(59) Bin, X. M.; Mischki, T. K.; Fan, C. Y.; Lopinski, G. P.; Wayner, D. D. M. *J. Phys. Chem. C* **2007**, *111*, 13547.

(60) Aureau, D.; Ozanam, F.; Allongue, P.; Chazalviel, J. N. *Langmuir* **2008**, *24*, 9440.

(61) Perring, M.; Dutta, S.; Arafat, S.; Mitchell, M.; Kenis, P. J. A.; Bowden, N. B. *Langmuir* **2005**, *21*, 10537.

(62) Faucheux, A.; Gouget-Laemmel, A. C.; de Villeneuve, C. H.; Boukherroub, R.; Ozanam, F.; Allongue, P.; Chazalviel, J. N. *Langmuir* **2006**, *22*, 153.

(63) Carey, F. A.; Sundberg, R. J. *Advanced Organic Chemistry Part A: Structure and Mechanisms*; 5th ed.; Springer: New York, 2008.

(64) de Lijser, H. J. P.; Snelgrove, D. W.; Dinnocenzo, J. P. *J. Am. Chem. Soc.* **2001**, *123*, 9698.

(65) Dinnocenzo, J. P.; Farid, S.; Goodman, J. L.; Gould, I. R.; Todd, W. P. *Mol. Cryst. Liq. Cryst.* **1991**, *194*, 151.

(66) Postigo, A.; Kopsov, S.; Ferreri, C.; Chatgilialoglu, C. *Org. Lett.* **2007**, *9*, 5159.

(67) Michalak, D. J.; Amy, S. R.; Aureau, D.; Dai, M.; Esteve, A.; Chabal, Y. J. *Nat. Mater.* **2010**, *9*, 266.

(68) Solares, S. D.; Michalak, D. J.; Goddard, W. A.; Lewis, N. S. *J. Phys. Chem. B* **2006**, *110*, 8171.

(69) Coletti, C.; Marrone, A.; Giorgi, G.; Sgamellotti, A.; Cerofolini, G.; Re, N. *Langmuir* **2006**, *22*, 9949.

(70) Kabalka, G. W.; Zhou, L. L.; Wang, L.; Pagni, R. M. *Tetrahedron* **2006**, *62*, 857.

(71) Becke, A. D. *J. Chem. Phys.* **1993**, *98*, 5648.

(72) Frisch, M. J., et al. *Gaussian 09*, Revision A.02, Gaussian, Inc.: Wallingford, CT, 2009.

(73) Kollegger, G.; Hassler, K. *J. Org. Chem.* **1995**, *485*, 233.

(74) Gilman, H.; Smith, C. L. *J. Org. Chem.* **1967**, *8*, 245.

(75) Apeloig, Y.; Yuzefovich, M.; Bendikov, M.; BravoZhivotovskii, D.; Klinkhammer, K. *Organometallics* **1997**, *16*, 1265.